J|A|C|S

A R T I C L E S

Living Polymerization of Ethylene Catalyzed by Titanium Complexes Having Fluorine-Containing Phenoxy−Imine Chelate Ligands

Makoto Mitani, Jun-ichi Mohri, Yasunori Yoshida, Junji Saito, Seiichi Ishii,
Kazutaka Tsuru, Shigekazu Matsui, Rieko Furuyama, Takashi Nakano,
Hidetsugu Tanaka, Shin-ichi Kojoh, Tomoaki Matsugi, Norio Kashiwa, and
Terunori Fujita*

*Contribution from the R & D Center, Mitsui Chemicals, Inc., 580-32 Nagaura, Sodegaura,
Chiba, 299-0265, Japan*

Received July 19, 2001

Abstract: Seven titanium complexes bearing fluorine-containing phenoxy−imine chelate ligands, TiCl$_2$-$\{\eta^2$-1-[C(H)=NR]-2-O-3-^{t}Bu-C$_6$H$_3\}_2$ [R = 2,3,4,5,6-pentafluorophenyl (**1**), R = 2,4,6-trifluorophenyl (**2**), R = 2,6-difluorophenyl (**3**), R = 2-fluorophenyl (**4**), R = 3,4,5-trifluorophenyl (**5**), R = 3,5-difluorophenyl (**6**), R = 4-fluorophenyl (**7**)], were synthesized from the lithium salt of the requisite ligand and TiCl$_4$ in good yields (22%−76%). X-ray analysis revealed that the complexes **1** and **3** adopt a distorted octahedral structure in which the two phenoxy oxygens are situated in the trans-position while the two imine nitrogens and the two chlorine atoms are located cis to one another, the same spatial disposition as that for the corresponding nonfluorinated complex. Although the Ti−O, Ti−N, and Ti−Cl bond distances for complexes **1** and **3** are very similar to those for the nonfluorinated complex, the bond angles between the ligands (e.g., O−Ti−O, N−Ti−N, and Cl−Ti−Cl) and the Ti−N−C−C torsion angles involving the phenyl on the imine nitrogen are different from those for the nonfluorinated complex, as a result of the introduction of fluorine atoms. Complex **1**/methylalumoxane (MAO) catalyst system promoted living ethylene polymerization to produce high molecular weight polyethylenes (M_n > 400 000) with extremely narrow polydispersities (M_w/M_n < 1.20). Very high activities (TOF > 20 000 min^{-1} atm^{-1}) were observed that are comparable to those of Cp$_2$ZrCl$_2$/MAO at high polymerization temperatures (25, 50 °C). Complexes **2**−**4**, which have a fluorine atom adjacent to the imine nitrogen, behaved as living ethylene polymerization catalysts at 50 °C, whereas complexes **5**−**7**, possessing no fluorine adjacent to the imine nitrogen, produced polyethylenes having M_w/M_n values of ca. 2 with β-hydrogen transfer as the main termination pathway. These results together with DFT calculations suggested that the presence of a fluorine atom adjacent to the imine nitrogen is a requirement for the high-temperature living polymerization, and the fluorine of the active species for ethylene polymerization interacts with a β-hydrogen of a polymer chain, resulting in the prevention of β-hydrogen transfer. This catalyst system was used for the synthesis of a number of unique block copolymers such as polyethylene-*b*-poly(ethylene-*co*-propylene) diblock copolymer and polyethylene-*b*-poly(ethylene-*co*-propylene)-*b*-syndiotactic polypropylene triblock copolymer from ethylene and propylene.

Introduction

There has been great interest in the discovery and development of high-performance living olefin polymerization catalysts based on soluble, well-defined transition metal complexes. This is because of the usefulness of living olefin polymerization techniques for the preparation of precisely controlled polymers such as monodisperse polymers, terminally functionalized polymers, and block copolymers, all of which are anticipated to possess novel properties and new uses as high-performance polymers. However, living olefin polymerization required low temperatures, normally below room temperature, to suppress the chain termination or transfer steps (e.g., β-hydride elimination, β-alkyl elimination, and chain transfer to a cocatalyst), and thus it generally exhibits low activity with insufficient molecular weight value, which has restricted the utility of this
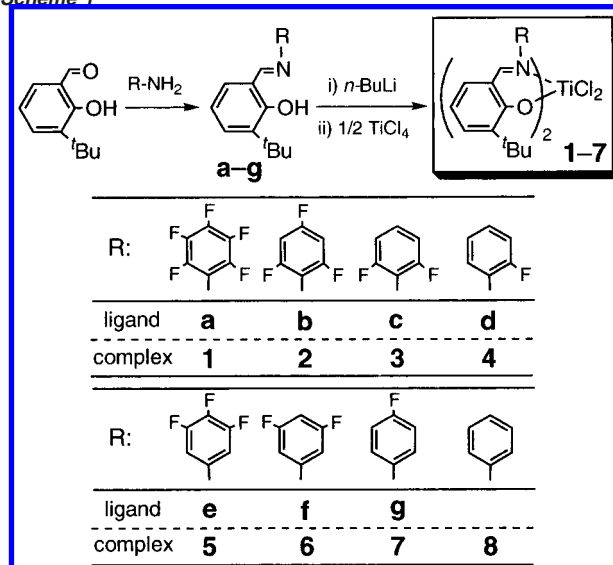
method. Recent research effort devoted to the study of soluble, well-defined transition metal complexes for olefin polymerization[1,2] has resulted in the introduction of a variety of high-performance catalysts for the living polymerization of olefins[3−15] such as ethylene, propylene, 1-hexene, and higher α-olefins. Some of the catalysts promote the room-temperature living polymerization of 1-hexene.[7] Some are active for stereospecific

(1) (a) Kaminsky, W.; Külper, K.; Brintzinger, H. H.; Wild, F. R. W. P. *Angew. Chem., Int. Ed. Engl.* **1985**, *97*, 507−508. (b) Kaminsky, W. *Catal. Today* **1994**, *20*, 257−271. (c) Möhring, P. C.; Coville, N. J. *J. Organomet. Chem.* **1994**, *479*, 1−29. (d) Brintzinger, H. H.; Fischer, D.; Mülhaupt, R.; Rieger, B.; Waymouth, R. M. *Angew. Chem., Int. Ed. Engl.* **1995**, *34*, 1143−1170. (e) Kaminsky, W.; Arndt, M.; *Adv. Polym. Sci.* **1997**, *127*, 144−187. (f) Coates, G. W. *Chem. Rev.* **2000**, *100*, 1223−1252.
(2) For recent reviews, see: (a) Britovsek, G. J. P.; Gibson, V. C.; Wass, D. F. *Angew. Chem., Int. Ed.* **1999**, *38*, 428−447. (b) Ittel, S. D.; Johnson, L. K.; Brookhart, M. *Chem. Rev.* **2000**, *100*, 1169−1203. And references were cited in ref 16i.

living polymerization of propylene[4–6] or 1-hexene.[9] In addition, others are capable of producing α-olefin-based block copolymers.[10] There are, however, a limited number of catalysts that promote room-temperature living ethylene polymerization.[11–15] Moreover, the preparation of well-defined ethylene-based block copolymers has not yet been reported.

Previously we developed, as a result of ligand-oriented catalyst design research, a new family of group 4 transition metal complexes possessing a pair of phenoxy−imine chelate ligands, named FI Catalysts,[16] that show exceptionally high ethylene polymerization activities. FI Catalysts have been found to produce various new polymers such as very low molecular weight polyethylenes and ethylene−propylene copolymers,

Scheme 1

(3) (a) Hagihara, H.; Shiono, T.; Ikeda, T. *Macromolecules* **1998**, *31*, 3184−3188. (b) Hasan, T.; Ioku, A.; Nishii, K.; Shiono, T.; Ikeda, T. *Macromolecules* **2001**, *34*, 3142−3145. (c) Fukui, Y.; Murata, M.; Soga, K. *Macromol. Rapid Commun.* **1999**, *20*, 637−640. (d) Turner, H. W.; Hlatky, G. G. Exxon, PCT International Application 9112285, 1991 *(Chem. Abstr.* **1992**, *116*, 61330t).
(4) (a) Doi, Y.; Keii, T. *Adv. Polym. Sci.* **1986**, *73−4*, 201−248. (b) Doi, Y.; Tokuhiro, N.; Soga, K. *Makromol. Chem., Macromol. Chem. Phys.* **1989**, *190*, 643−651 and references therein.
(5) Tian, J.; Hustad, P. D.; Coates, G. W. *J. Am. Chem. Soc.* **2001**, *123*, 5134−5135.
(6) (a) Saito, J.; Mitani, M.; Mohri, J.; Ishii, S.; Yoshida, Y.; Matsugi, T.; Kojoh, S.; Kashiwa, N.; Fujita, T. *Chem. Lett.* **2001**, 576−577. (b) Kojoh, S.; Matsugi, T.; Saito, J.; Mitani, M.; Fujita, T.; Kashiwa, N. *Chem. Lett.* **2001**, 822−823. (c) Saito, J.; Mitani, M.; Onda, M.; Mohri, J.; Ishii, S.; Yoshida, Y.; Nakano, T.; Tanaka, H.; Matsugi, T.; Kojoh, S.; Kashiwa, N.; Fujita, T. *Macromol. Rapid Commun.* **2001**, *22*, 1072−1075.
(7) (a) Scollard, J. D.; McConville, D. H. *J. Am. Chem. Soc.* **1996**, *118*, 10008−10009. (b) Scollard, J. D.; McConville, D. H.; Vittal, J. J.; Payne, N. C. *J. Mol. Catal. A.* **1998**, *128*, 201−214.
(8) (a) Baumann, R.; Davis, W. M.; Schrock, R. R. *J. Am. Chem. Soc.* **1997**, *119*, 3830−3831. (b) Liang, L. C.; Schrock, R. R.; Davis, W. M.; McConville, D. H. *J. Am. Chem. Soc.* **1999**, *121*, 5797−5798. (c) Mehrkhodavandi, M.; Schrock, R. R. *J. Am. Chem. Soc.* **2001**, *123*, 10746−10747. (d) Y.-M. Jeon, S. J. Park, J. Heo, K. Kim, *Organometallics* **1998**, *17*, 3161−3163. (e) Tshuva, E. Y.; Goldberg, I.; Kol, M.; Goldschmidt, Z. *Inorg. Chem. Commun.* **2000**, *3*, 611−614.
(9) (a) Jayaratne, K. C.; Sita, L. R. *J. Am. Chem. Soc.* **2000**, *122*, 958−959. (b) Jayaratne, K. C.; Keaton, R. J.; Henningsen, D. A.; Sita, L. R. *J. Am. Chem. Soc.* **2000**, *122*, 10490−10491. (c) Keaton, R. J.; Jayaratne, K. C.; Henningsen, D. A.; Koterwas, L. A.; Sita, L. R. *J. Am. Chem. Soc.* **2001**, *123*, 6197−6198. (d) Jayaratne, K. C.; Sita, L. R. *J. Am. Chem. Soc.* **2001**, *123*, 10754−10755.
(10) (a) Johnson, L. K.; Killian, C. M.; Brookhart, M. *J. Am. Chem. Soc.* **1995**, *117*, 6414−6415. (b) Killian, C. M.; Tempel, D. J.; Johnson, L. K.; Brookhart, M. *J. Am. Chem. Soc.* **1996**, *118*, 11664−11665.
(11) Yasuda, H.; Furo, M.; Yamamoto, H.; Nakamura, A.; Miyake, S.; Kibino, N. *Macromolecules* **1992**, *25*, 5115−5116.
(12) (a) Mashima, K.; Fujikawa, S.; Nakamura, A. *J. Am. Chem. Soc.* **1993**, *115*, 10990−10991. (b) Mashima, K.; Fujikawa, S.; Urata, H.; Tanaka, E.; Nakamura, A. *J. Chem. Soc., Chem. Commun.* **1994**, 1623−1624. (c) Mashima, K.; Fujikawa, S.; Tanaka, Y.; Urata, H.; Oshiki, T.; Tanaka, E.; Nakamura, A. *Organometallics* **1995**, *14*, 2633−2640.
(13) Brookhart, M.; DeSimone, J. M.; Grant, B. E.; Tanner, M. J. *Macromolecules* **1995**, *28*, 5378−5380.
(14) Gottfried, A. C.; Brookhart, M. *Macromolecules* **2001**, *34*, 1140−1142.
(15) Matsugi, T.; Matsui, S.; Kojoh, S.; Takagi, Y.; Inoue, Y.; Fujita, T.; Kashiwa, N. *Chem. Lett.* **2001**, 566−567.
(16) (a) Fujita, T.; Tohi, Y.; Mitani, M.; Matsui, S.; Saito, J.; Nitabaru, M.; Sugi, K.; Makio, H.; Tsutsui, T. Europe Patent, EP-0874005, 1998 *(Chem. Abstr.* **1998**, *129*, 331166). (b) Matsui, S.; Tohi, Y.; Mitani, M.; Saito, J.; Makio, H.; Tanaka, H.; Nitabaru, M.; Nakano, T.; Fujita, T. *Chem. Lett.* **1999**, 1065−1066. (c) Matsui, S.; Mitani, M.; Saito, J.; Tohi, Y.; Makio, H.; Tanaka, H.; Fujita, T. *Chem. Lett.,* **1999** 1263−1264. (d) Matsui, S.; Mitani, M.; Saito, J.; Matsukawa, N.; Tanaka, H.; Nakano, T.; Fujita, T. *Chem. Lett.* **2000**, 554−555. (e) Saito, J.; Mitani, M.; Matsui, S.; Kashiwa, N.; Fujita, T. *Macromol. Rapid Commun.* **2000**, *21*, 1333−1336. (f) Matsui, S.; Fujita, T. *Catal. Today* **2001**, *66*, 63−73. (g) Yoshida, Y.; Matsui, S.; Takagi, Y.; Mitani, M.; Nitabaru, M.; Nakano, T.; Tanaka, H.; Fujita, T. *Chem. Lett.* **2000**, 1270−1271. (h) Matsukawa, N.; Matsui, S.; Mitani, M.; Saito, J.; Tsuru, K.; Kashiwa, N.; Fujita, T. *J. Mol. Catal. A* **2001**, *169*, 99−104. (i) Matsui, S.; Mitani, M.; Saito, J.; Tohi, Y.; Makio, H.; Matsukawa, N.; Takagi, Y.; Tsuru, K.; Nitabaru, M.; Nakano, T.; Tanaka, H.; Kashiwa, N.; Fujita, T. *J. Am. Chem. Soc.* **2001**, *123*, 6847−6856. (j) Saito, J.; Mitani, M.; Matsui, S.; Tohi, Y.; Makio, H.; Nakano, T.; Tanaka, H.; Kashiwa, N.; Fujita, T. *Macromol. Chem. Phys.* **2002**, *203*, 59−65. (k) Ishii, S.; Saito, J.; Mitani, M.; Mohri, J.; Matsukawa, N.; Tohi, Y.; Matsui, S.; Kashiwa, N.; Fujita, T. *J. Mol. Catal. A* **2002**, *179*, 11−16. (l) Yoshida, Y.; Matsui, S.; Takagi, Y.; Mitani, M.; Nakano, T.; Tanaka, H.; Kashiwa, N.; Fujita, T. *Organometallics* **2001**, *20*, 4793−4799. (m) Tian, J.; Coates, G. W. *Angew. Chem., Int. Ed.* **2000**, *39*, 3626−3629.

ultrahigh molecular weight polyethylenes and ethylene−propylene copolymers,[16i] and high molecular weight poly-1-hexenes having an atactic structure with considerable regioirregular units.[16e] Further studies on the FI Catalysts having heteroatom(s) and/or heteroatom-containing substituent(s) in the ligand have led to the discovery of a new series of FI Catalysts having fluorine atom(s) in the ligand that display unprecedented catalytic performance for the living polymerization of ethylene.[17] In this contribution, we report the syntheses, structures, and ethylene polymerization behavior of FI Catalysts having fluorine-containing ligand and introduce a new breakthrough for achieving high-temperature living ethylene polymerization. In addition, we describe the preparation of di- and triblock copolymers in order to demonstrate the usefulness of the catalysts for the synthesis of the desired precisely controlled polymers.

Results and Discussion

Synthesis of Titanium Complexes Having Fluorine-Containing Phenoxy−Imine Chelate Ligands. A general synthetic route for the titanium complexes employed in this study, bis[*N*-(3-*tert*-butylsalicylidene)fluoroanilinato]titanium(IV) dichloride **1−7**, is depicted in Scheme 1. The fluorine-containing phenoxy−imine chelate ligands (**a−g**), *N*-(3-*tert*-butylsalicylidene)fluoroaniline, are synthesized in high yields (82−98%) by the Schiff base condensation of the corresponding fluorine-containing aniline with 3-*tert*-butylsalicylaldehyde using an acid as a catalyst. The desired titanium complexes **1−7** are prepared in moderate to good yields (22−76%) by the reaction of TiCl₄ with 2 equiv of the lithium salt of the fluorine-containing phenoxy-imine ligands in dried diethyl ether. The overall yields starting from commercially available 3-*tert*-butylsalicylaldehyde are fairly good.

X-ray Analyses of Complexes 1 and 3. The molecular structures of complexes **1** and **3** were determined by X-ray

(17) (a) Mitani, M.; Yoshida, Y.; Mohri, J.; Tsuru, K.; Ishii, S.; Kojoh, S.; Matsugi, T.; Saito, J.; Matsukawa, N.; Matsui, S.; Nakano, T.; Tanaka, H.; Kashiwa, N.; Fujita, T. WO Pat. 01/55231 A1, 2001. (b) Fujita, T.; Mitani, M.; Matsui, S.; Saito, J.; Yoshida, Y.; Tohi, Y.; Matsukawa, N.; Ishii, S.; Mohri, J.; Inoue, Y.; Nakano, T.; Tanaka, H.; Matsugi, T.; Kojoh, S.; Kashiwa, N. *International Symposium on Future Technology for Olefin and Olefin Polymerization Catalysis, proceedings,* Tokyo, March 2001, Abstr. No. OP-21. (c) Saito, J.; Mitani, M.; Mohri, J.; Yoshida, Y.; Matsui, S.; Ishii, S.; Kojoh, S.; Kashiwa, N.; Fujita, T. *Angew. Chem., Int. Ed.* **2001**, *40*, 2918−2920.
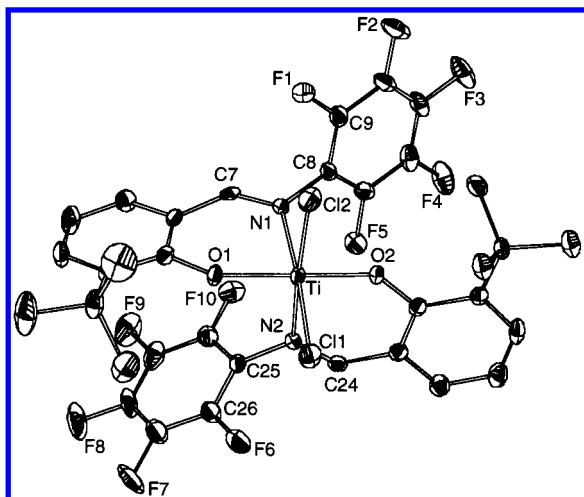
Figure 1. Molecular structure of complex **1** with thermal ellipsoids at 50% probability level.
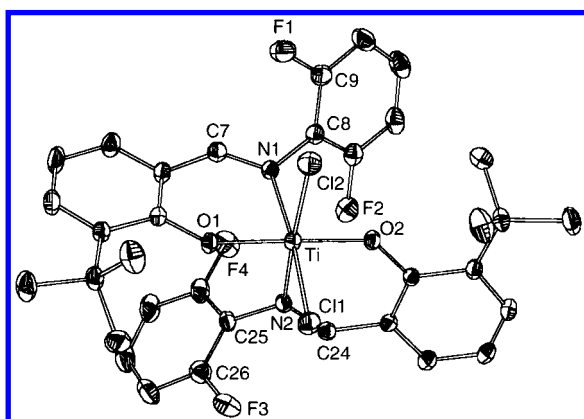
Figure 2. Molecular structure of complex **3** with thermal ellipsoids at 30% probability level.

Table 1. Selected Bond Distances (Å), Angles (deg), and Torsion Angles (deg) for Complexes **1**, **3**, and **8**

complex	1	3	8
Bond Distances			
Ti−Cl(1)	2.2876(7)	2.2799(9)	2.296(2)
Ti−Cl(2)	2.2578(8)	2.2811(9)	2.305(1)
Ti−O(1)	1.841(1)	1.848(2)	1.851(3)
Ti−O(2)	1.845(1)	1.872(2)	1.852(3)
Ti−N(1)	2.234(2)	2.218(2)	2.213(4)
Ti−N(2)	2.217(2)	2.217(2)	2.236(4)
N(1)−C(7)	1.298(3)	1.298(3)	1.286(6)
N(2)−C(24)	1.296(3)	1.289(3)	1.295(6)
N(1)−C(8)	1.437(3)	1.435(3)	1.441(5)
N(2)−C(25)	1.428(3)	1.451(3)	1.443(6)
Bond Angles			
Cl(1)−Ti−Cl(2)	96.42(3)	98.09(4)	103.11(6)
O(1)−Ti−O(2)	163.61(6)	166.99(8)	171.6(1)
N(1)−Ti−N(2)	86.94(7)	86.18(8)	76.4(1)
Torsion Angles			
Ti−N(1)−C(8)−C(9)	−95.5(2)	−106.7(3)	−76.9(5)
Ti−N(2)−C(25)−C(26)	−85.3(3)	−93.5(3)	−63.2(5)

crystallography. The structures are shown in Figures 1 and 2, while key bond distances and angles, together with those for the corresponding nonfluorinated complex **8**,[16j] are summarized in Table 1. The X-ray structures of complexes **1** and **3** feature a distorted octahedral complex in which the titanium is bound to two cis-coordinated [O, N] chelating ligands (the oxygen atoms being situated in the trans-position) and the two chlorine

atoms (being situated in the cis-position). Therefore, the spatial arrangement of complexes **1** and **3** is the same as that of complex **8**. Assuming that two chlorine-bound sites are transformed to olefin polymerization sites while retaining their stereochemical cis-relationship, active species for olefin polymerization, derived from complexes **1** and **3,** possess two available cis-located sites convenient for olefin polymerization. Although the Ti−O, Ti−N, and Ti−Cl bond distances for complexes **1** and **3** are very similar to those for nonfluorinated complex **8**, the bond angles between the ligands (e.g., O−Ti−O, N−Ti−N, and Cl−Ti−Cl) are different compared with those for complex **8**. Complexes **1** and **3** have the narrower Cl−Ti−Cl and O−Ti−O angles and wider N−Ti−N angle relative to those for complex **8**. In addition, complexes **1** and **3** possess wider Ti−N−C−C torsion angles involving the phenyl on the imine nitrogen than complex **8**. These differences in the angles probably originate from the steric repulsion between the fluorine adjacent to the imine nitrogen and the *tert*-butyl group in the phenoxy benzene rings and electronic repulsion between the fluorine adjacent to the imine nitrogen and the chlorine atoms bound to the titanium metal. Since the F atoms are situated near Cl atoms, potential olefin polymerization sites, the F atoms are expected to affect the olefin polymerization process.

Living Ethylene Polymerization Promoted by the Complex 1/MAO System. Ethylene polymerizations with complex **1** and a typical metallocene, Cp_2ZrCl_2, as a comparison, using methylalumoxane (MAO) as a cocatalyst, were carried out at 25, 50, and 75 °C under atmospheric pressure. The results are collected in Table 2. At 25 °C the activity of the complex **1**/MAO catalyst system was found to be competitive with Cp_2ZrCl_2/MAO (entries 1, 2, 7). Thus, complex **1** displayed very high activities (TOF values: entry 1, 21 200 min^{-1} atm^{-1}; entry 2, 20 200 min^{-1} atm^{-1}), the activities being comparable to that exhibited by Cp_2ZrCl_2 (TOF value: entry 7, 18 400 min^{-1} atm^{-1}). It is noteworthy that the polyethylenes produced with complex **1**/MAO possess extremely narrow polydispersities (M_w/M_n = 1.15, 1.13) and high molecular weights (M_n = 191 000, 412 000). In addition, the M_n value and polymer yield obtained at 1 min polymerization (entry 2) is practically twice that for 0.5 min polymerization (entry 1). These results suggest that the ethylene polymerization catalyzed by complex **1**/MAO catalyst system proceeds in a living fashion, though Cp_2ZrCl_2/MAO produced polyethylenes having M_w/M_n values of ca. 2, typical value for nonliving system, under the same conditions. The M_n (>400 000) represents one of the highest values and, at the same time, the TOF value (>20 000 min^{-1} atm^{-1}) is also one of the highest activities for living ethylene polymerizations. In fact, the activities displayed by complex **1**/MAO are 3 orders of magnitude larger than those for the known living ethylene polymerization catalyst systems (TOF values, ca. 20 min^{-1} atm^{-1}). To the best of our knowledge, this is the first example of an exceptionally high-speed room-temperature living ethylene polymerization that produces very high molecular weight polyethylene with narrow polydispersity (M_w/M_n < 1.20). Melting temperatures (T_m) of the produced polyethylenes were 137 °C (entry 1) and 135 °C (entry 2), respectively, and ^{13}C NMR analyses of the polymers indicate that the polyethylenes have linear structures with virtually no branching. Generally, an increase in temperature for living polymerization causes chain transfers, resulting in the loss of living character. Surprisingly,

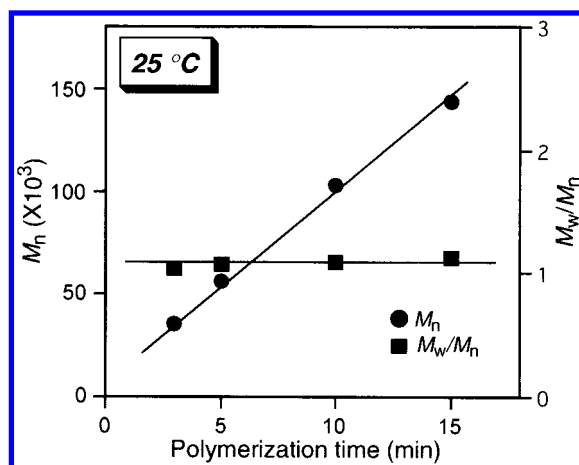**Table 2.** Results of Ethylene Polymerization with Complex **1**/MAO[a]

entry	complex (μmol)	temp (°C)	time (min)	polymer yield (g)	TOF (min^{-1}·atm^{-1})	$M_n{}^b$ (×10^3)	$M_w/M_n{}^b$
1	**1** (0.5)	25	0.5	0.149	21 200	191	1.15
2	**1** (0.5)	25	1	0.283	20 200	412	1.13
3	**1** (0.5)	50	0.5	0.172	24 500	257	1.08
4	**1** (0.5)	50	1	0.302	21 500	424	1.13
5	**1** (1.0)	75	0.5	0.247	17 600	214	1.09
6	**1** (1.0)	75	1	0.453	16 100	329	1.15
7	Cp$_2$ZrCl$_2$ (0.5)	25	1	0.258	18 400	157	1.73
8	Cp$_2$ZrCl$_2$ (0.5)	50	1	0.433	30 900	136	2.26

[a] Conditions: MAO cocatalyst (1.25 mmol), 1 atm, ethylene feed 100 L/h, 250 mL toluene. [b] Determined by GPC using polyethylene calibration.

Table 3. Results of Ethylene Polymerization with Complex **1**/MAO Using Diluted Ethylene and Various Polymerization Temperatures[a]
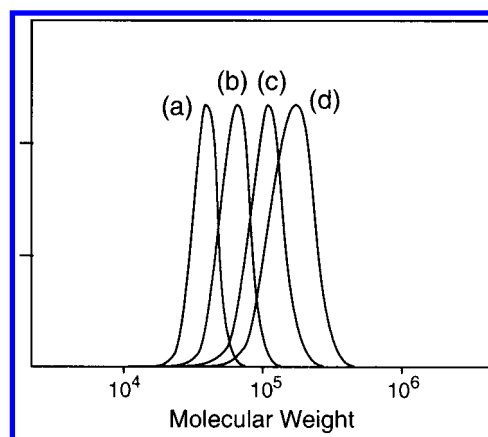
	$T = 25$ °C			$T = 50$ °C			$T = 75$ °C		
time (min)	polymer yield (g)	$M_n{}^b$ (×10^3)	$M_w/M_n{}^b$	polymer yield (g)	$M_n{}^b$ (×10^3)	$M_w/M_n{}^b$	polymer yield (g)	$M_n{}^b$ (×10^3)	$M_w/M_n{}^b$
3	0.027	35	1.05						
5	0.059	56	1.07	0.049	54	1.06	0.052	82	1.30
10	0.113	103	1.09	0.100	95	1.14	0.122	135	1.65
15	0.175	144	1.13	0.150	137	1.19	0.131	160	2.05

[a] Conditions: 1.0 μmol **1**, 1.25 mmol MAO cocatalyst, 1 atm, ethylene/N$_2$ feed 2 L/50 L/h (25, 50 °C), 5 L/50 L/h (75 °C), 250 mL toluene. [b] Determined by GPC using polyethylene calibration.

Figure 3. Plots of M_n and M_w/M_n as a function of polymerization time for ethylene polymerization with complex **1**/MAO at 25 °C.

Figure 4. GPC profile of polyethylenes obtained by complex **1**/MAO at 25 °C: (a) 3 min, $M_n = 35\,000$, $M_w/M_n = 1.05$ (b) 5 min, $M_n = 56\,000$, $M_w/M_n = 1.07$ (c) 10 min, $M_n = 103\,000$, $M_w/M_n = 1.09$ (d) 15 min, $M_n = 144\,000$, $M_w/M_n = 1.13$.

as presented in Table 2 (entries 3−6) the complex **1**/MAO catalyst system produced polyethylenes having extremely narrow polydispersities ($M_w/M_n = 1.08$−1.15) even at 50 and 75 °C. The temperature tolerance for performing living polymerization is exceptionally high compared with the known living polymerization systems, and therefore, it is of great significance.

To further confirm the living nature of the catalyst system, M_n and M_w/M_n values for complex **1**/MAO at 25 °C were monitored as a function of polymerization time. Since complex **1**/MAO is highly active for ethylene polymerization, long polymerization time may cause undesirable broadening of MWD, because of nonhomogenity of the polymerization system due to excess polymer precipitation. Consequently, we carried out polymerizations using diluted ethylene with nitrogen under atmospheric pressure. As shown in Table 3 and Figure 3, a linear relationship between M_n and polymerization time as well as narrow M_w/M_n values for all runs ($M_w/M_n = 1.05$−1.13) were found. Moreover, GPC peaks of the produced polyethylene shifted to higher molecular weight region with an increase in polymerization time while the monomodal shape was retained, and no shoulder peak and/or low molecular weight tail was detected during the course of the polymerization (Figure 4). The

molecular weight of the polyethylene was close to that calculated from the monomer/initiator ratio obtained from the mass of the polyethylene produced, showing that catalyst efficiency is substantially quantitative. These results clearly indicate that this catalyst system promotes highly controlled living ethylene polymerization at room temperature.

To investigate the living nature of the system at higher temperatures, M_n and M_w/M_n values vs polymerization time were plotted for the ethylene polymerization performed at 50 and 75 °C using the same polymerization method. As a result, at 50 °C, a linear relationship between M_n and polymerization time as well as narrow MWD values for all runs ($M_w/M_n = 1.06$−1.19) were found (Figure 5). On the other hand, at 75 °C, long polymerization time resulted in broad polydispersities, indicating that chain termination or transfer and/or catalyst deactivation was not negligible at the temperature (Figure 6). However, the M_n value of the polymer increased with increase in polymerization time, and therefore, complex **1**/MAO still possessed some characteristics of living polymerization at 75 °C. Considering that MAO is a potential chain transfer agent and, thus, normally living olefin polymerization can only be achieved using a borate
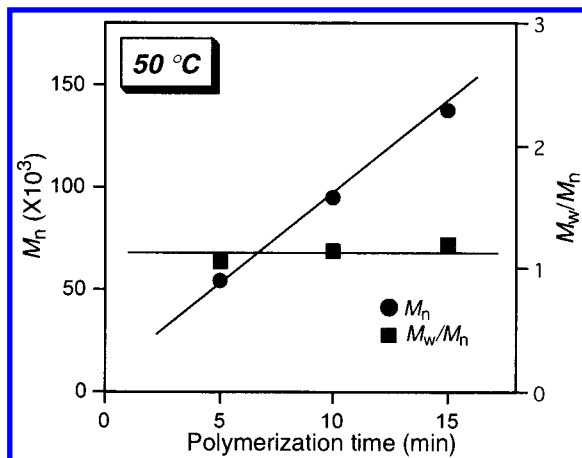
Figure 5. Plots of M_n and M_w/M_n as a function of polymerization time for ethylene polymerization with complex **1**/MAO at 50 °C.
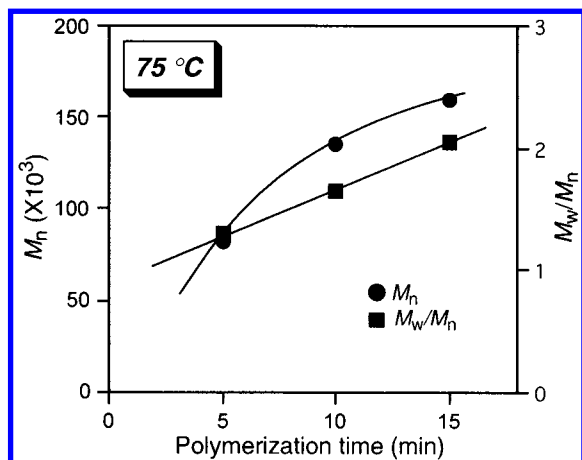
Figure 6. Plots of M_n and M_w/M_n as a function of polymerization time for ethylene polymerization with complex **1**/MAO at 75 °C.

cocatalyst in place of MAO, the living polymerization exhibited by complex **1**/MAO at high temperatures is significant.

Mechanistic Studies on the Living Ethylene Polymerization. Because the corresponding nonfluorinated titanium complex (**8**) does not promote living ethylene polymerization under similar conditions,[18] we postulated that the fluorine atom(s) in the ligand is responsible for the high-temperature living polymerization. Consequently, we conducted further research on the catalysis of titanium complexes possessing fluorine-containing phenoxy-imine chelate ligands in order to investigate the role of fluorine atom(s). To this end, six titanium complexes (**2**−**7**) having fluorinated ligands were prepared and investigated for their potential as ethylene polymerization catalysts at 50 °C. A summary of the ethylene polymerization behavior of complexes **2**−**7** is shown in Table 4.

Complexes **2**−**7** are active toward ethylene polymerization and produce solid polyethylenes. Catalytic activities and polydispersities of the produced polyethylenes are greatly affected by the number and the location of the fluorine atom(s) in the ligand. A comparison of the catalytic activities in Table 4 indicates that the complexes having a F atom adjacent to the

(18) As reported in ref 16b, the corresponding nonfluorinated complex **8** produced polyethylene having an M_w/M_n value of ca. 2.0. However, the complex possesses some characteristics of living ethylene polymerization for short time at room temperature, though it displays much lower catalytic performance compared with complex **1**.

Table 4. Results of Ethylene Polymerization with Complexes **2**−**7**/MAO[a]

entry	complex	polymer yield (g)	TOF (min$^{-1} \cdot$atm^{-1})	$M_n{}^b$ ($\times 10^3$)	$M_w/M_n{}^b$
1	**2**	0.081	1440	145	1.25
2	**3**	0.069	492	64	1.05
3	**4**	0.053	76	13	1.06
4	**5**	0.372	26500	98	1.99
5	**6**	0.267	19000	129	1.78
6	**7**	0.177	3160	128	2.18

[a] Conditions: catalyst (0.4 μmol for entries 1, 6; 1.0 μmol for entry 2; 5.0 μmol for entry 3; 0.5 μmol for entries 4, 5), time (5 min for entries 1, 2, 3, 6; 1 min for entries 4, 5), MAO cocatalyst (1.25 mmol), 50 °C, 1 atm, ethylene feed 100 L/h, 250 mL toluene. [b] Determined by GPC using polyethylene calibration.
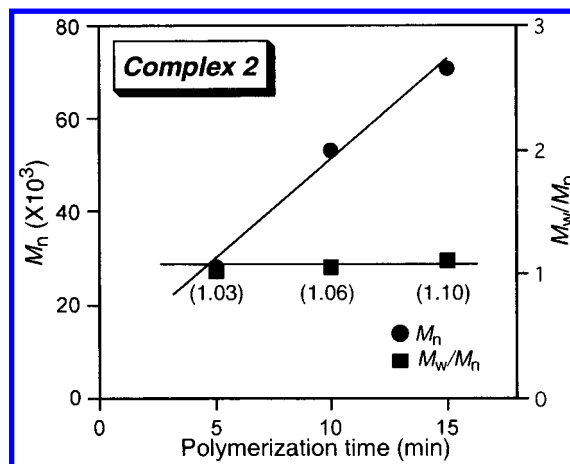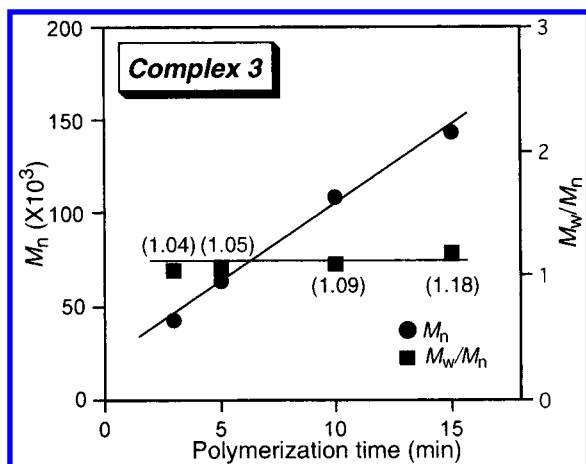

Figure 7. Plots of M_n and M_w/M_n vs polymerization time with complex **2**/MAO (2.0 μmol catalyst, 1.25 mmol MAO, ethylene/N$_2$ 10 L/50 L/h, 50 °C).

imine nitrogen, complexes **2**−**4**, display lower activities (TOF: **2**, 1440 min^{-1} atm^{-1}; **3**, 492 min^{-1} atm^{-1}; **4**, 76 min^{-1} atm^{-1}) relative to the complexes having the same number of F atoms with no fluorine adjacent to the imine nitrogen, complexes **5**−**7** (TOF: **5**, 26 500 min^{-1} atm^{-1}; **6**, 19 000 min^{-1} atm^{-1}; **7**, 3160 min^{-1} atm^{-1}), suggesting that the fluorine adjacent to the imine nitrogen suppresses polymerization. The catalytic activities increased with an increase in the number of F atom in the ligand (TOF, **2** > **3** > **4** and **5** > **6** > **7**), being probably ascribed to the electron-withdrawing nature of fluorine, resulting in a more electrophilic titanium center.
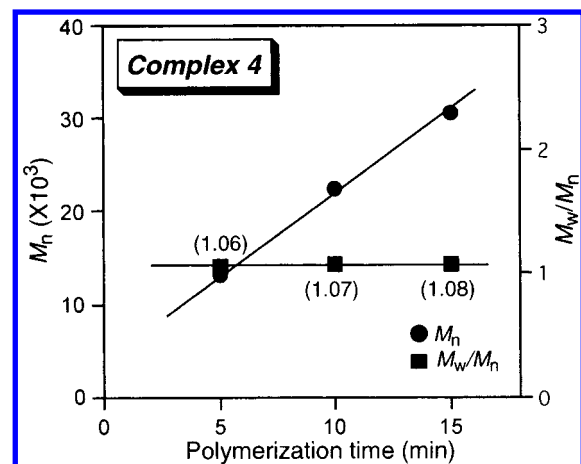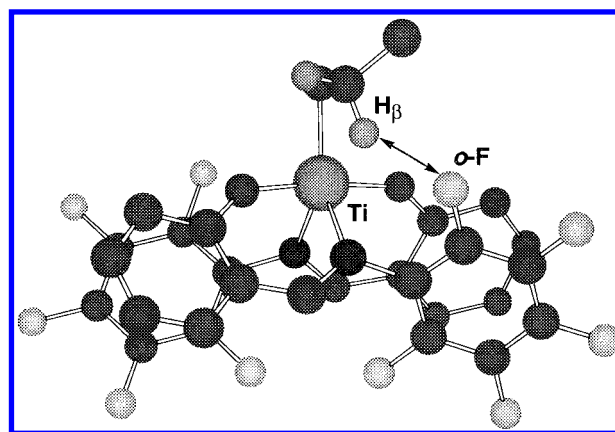
It is significant to note that the polyethylenes produced by complexes **2**−**4** with fluorine atom(s) adjacent to the imine nitrogen possess narrow polydispersites (M_w/M_n: **2**, 1.25; **3**, 1.05; **4**, 1.06). The polydispersities suggest that the polymerizations promoted by complexes **2**−**4** may proceed through a living mechanism. A linear increase in M_n vs polymerization time together with the narrow polydispersity for all runs at 50 °C (M_w/M_n: **2**, 1.03−1.10; **3**, 1.04−1.18; **4**, 1.06−1.08) (Figures 7−9) confirms that the polymerizations exhibited by complexes **2**−**4** are living.

Alternatively, the polydispersities of the polyethylenes formed with complexes **5**−**7** with no fluorine adjacent to the imine nitrogen are 1.99, 1.78, and 2.18, respectively, being comparable to the values obtained with common metallocene catalysts. Therefore, complexes **5**−**7** did not promote living polymerization of ethylene under the conditions employed. The polymerization behavior of complexes **1**−**7** clearly indicates that the presence of a F atom adjacent to the imine nitrogen in the ligand

Figure 8. Plots of M_n and M_w/M_n vs polymerization time with complex **3**/MAO (1.0 μmol catalyst, 1.25 mmol MAO, ethylene 100 L/h, 50 °C).

Figure 9. Plots of M_n and M_w/M_n vs polymerization time with complex **4**/MAO (5.0 μmol catalyst, 1.25 mmol MAO, ethylene 100 L/h, 50 °C).
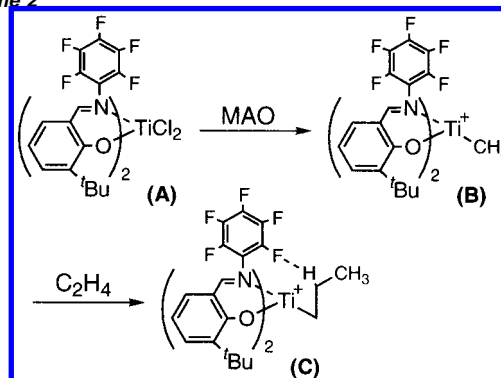
is a requirement for the high-temperature living polymerization. IR analyses of the polyethylenes produced by nonliving type complexes **5**−**7** reveal a vinyl end group concentration of ca. 0.1 per 1000 carbon atoms, showing that β-hydrogen transfer is the main termination pathway for the nonliving type complexes. Therefore, the fluorine adjacent to the imine nitrogen is thought to suppress the β-hydrogen transfer.[19]

As reported, DFT calculations are an effective tool for analyzing the structure of group 4 transition metal complexes bearing two phenoxy imine chelate ligands.[16i] Since the predicted structures for complexes **1** and **3** using DFT calculations were consistent with those elucidated by the X-ray analyses (see the Supporting Information), DFT calculations are also effective in analyzing the structures of titanium complexes bearing fluorine-containing phenoxy-imine chelate ligands. The catalytically active species derived from group 4 transition metal complexes is now widely regarded to be an alkyl cationic complex[20] (Scheme 2), and thus, DFT calculations were performed on the alkyl cationic complexes derived from
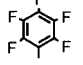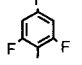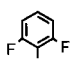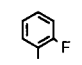
(19) DFT calculations suggest that chain transfer to monomer or to Al is sterically unfavorable for the complexes employed in this study.
(20) (a) Hlatky, G. G.; Turner, H. W.; Eckman, R. R. *J. Am. Chem. Soc.* **1989**, *111*, 2728−2729. (b) Jordan, R. F. *Adv. Organomet. Chem.* **1991**, *32*, 325−387. (c) Sishta, C.; Hathorn, R. M.; Marks, T. J. *J. Am. Chem. Soc.* **1992**, *114*, 1112−1114. (d) Yang, X.; Stern, C. L.; Marks, T. J. *J. Am. Chem. Soc.* **1994**, *116*, 10015−10031. (e) Bochmann, M. *J. Chem. Soc., Dalton Trans.* **1996**, 255−270.

Figure 10. Structure of an active species (**C**) derived from complex **1** calculated by DFT. *t*Bu groups are omitted for clarity.

Scheme 2

Table 5. F−H$_\beta$ Interactions Calculated by DFT

R:	F F / F F	F / F F	F / F	F
complex	**1**	**2**	**3**	**4**
$r(F-H_\beta)^a$	2.276	2.362	2.346	2.324
$q(F)^b$	-0.466	-0.470	-0.476	-0.482
$q(H_\beta)^c$	0.095	0.108	0.111	0.117
$ES(F-H_\beta)^d$	-27.1	-29.9	-31.2	-33.6

[a] F−H$_\beta$ distance (Å). [b] Mulliken charge of the nearest *o*-F to H$_\beta$. [c] Mulliken charge of H$_\beta$. [d] Electrostatic energy for F−H$_\beta$ interaction (kJ/mol).

complexes **1**−**4** (**C**, *n*-propyl; model for polymer chain) to investigate the role of the fluorine for the living polymerization. And the structure of an active species (**C**) derived from complex **1** is shown in Figure 10. The calculation results suggest that the fluorine adjacent to the imine nitrogen of the active species for ethylene polymerization interacts with a β-hydrogen of a polymer chain (F−H$_\beta$ distance: **1**, 2.276 Å; **2**, 2.362 Å; **3**, 2.346 Å; **4**, 2.324 Å) (Table 5).[21] In addition, electrostatic energy values between the fluorine adjacent to the imine nitrogen and the β-hydrogen were estimated to be ca. −30 kJ/mol based on the calculation results, further confirming the interaction between the fluorine and the β-hydrogen. The interaction between the

(21) The C−H bond length is considerably elongated (1.113 Å) by the strong interaction between the β-hydrogen and the *o*-fluorine, though the C−F bond length is practically the same.
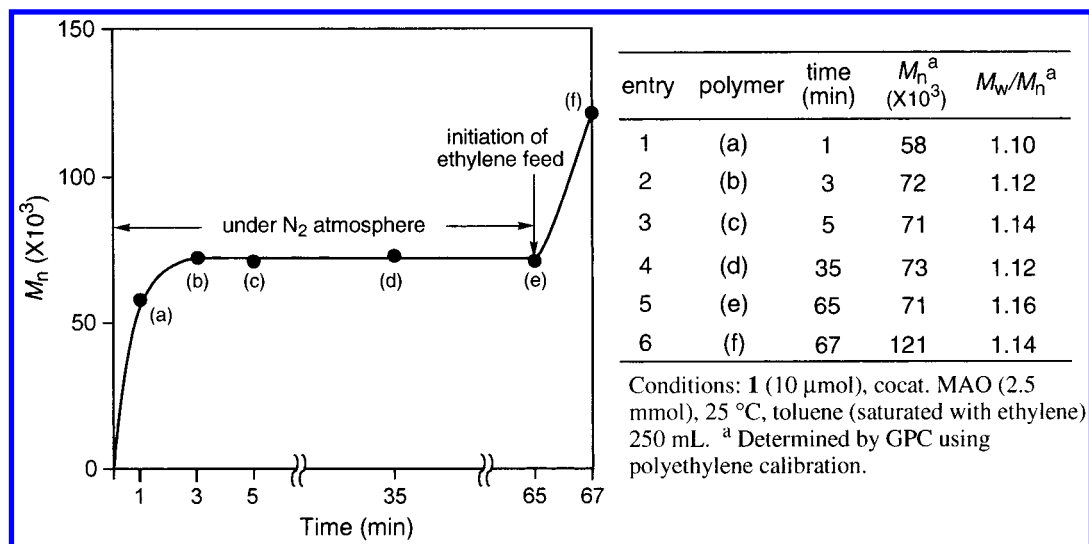
Figure 11. Plots of M_n vs polymerization time with complex **1**/MAO using the postpolymerization method.
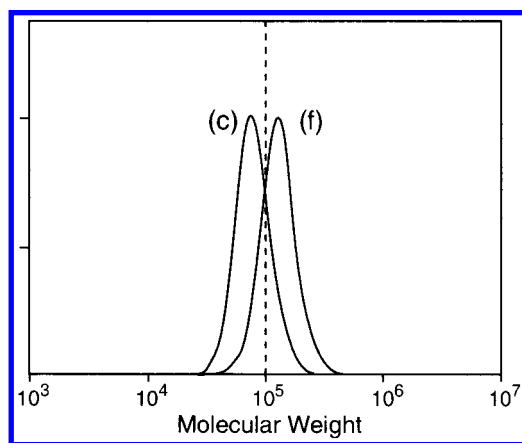

Figure 12. GPC profile of polyethylenes obtained with the postpolymerization method; polymer (c) and polymer (f).

fluorine and the β-hydrogen probably mitigates the reactivity of the β-hydrogen toward the titanium metal and/or a coordinated ethylene, resulting in the prevention of β-hydrogen transfer.[22] The interaction may provide a new breakthrough for achieving high-temperature living ethylene polymerization.

Application of Complex 1/MAO to the Synthesis of Block Copolymers. First, we investigated the stability of "living" polymer chain in the absence of reacting monomers, which affects the application of the catalyst system to the preparation of block copolymers.

Thus, treatment of complex **1**/MAO with ethylene-saturated toluene at room temperature under nitrogen atmosphere for 65 min (the ethylene was substantially consumed within 3 min as indicated by Figure 11, entries 2 and 3) and then the ethylene gas feed (20 L/h, 2 min) to the polymerization system resulted in the formation of polyethylene having narrow polydispersity ($M_w/M_n = 1.14$) (GPC traces of polymer c and f are shown in Figure 12). Therefore, there is practically no chain termination or transfer operative in the complex **1**/MAO catalyst system at

least for 60 min, even in the absence of ethylene, indicating the high potential of the system for the synthesis of ethylene-based block copolymers.

Because the known living olefin polymerization catalysts generally promote the living polymerization of either ethylene or α-olefins such as propylene and 1-hexene, the preparation of ethylene-based block copolymers remains a challenge. Accordingly, we decided to synthesize block copolymers from ethylene and propylene since, as reported previously, complex **1**/MAO promotes the room-temperature living polymerization of propylene in addition to ethylene to produce highly syndiotactic monodisperse polypropylene.[6,17a] A new A−B diblock copolymer, polyethylene-*b*-syndiotactic polypropylene, was prepared from ethylene and propylene by the sequential monomer addition (Table 6, entry 1). Thus, ethylene gas (100 L/h) was introduced to toluene in a reactor. After 5 min, the ethylene gas feed was stopped and the system was kept under nitrogen atmosphere. Complex **1** and MAO were added to the reactor to prepare a polyethylene (PE) segment. After 5 min, the propylene gas feed (30 L/h, 300 min) was initiated to create a sequential syndiotactic polypropylene (sPP) segment. The monomodal GPC curves for the PE A block ($M_n = 115\,000$, $M_w/M_n = 1.10$) and the final PE-*b*-PP A−B diblock ($M_n = 136\,000$, $M_w/M_n = 1.15$) indicate a shift toward higher molecular weight range while narrow polydispersity is retained, demonstrating the creation of the desired block copolymer. The block copolymer possesses a propylene content of 16.1 mol % (from NMR analysis), the value being in accordance with the increased molecular weight for the sPP segment. This is probably the first synthesis of well-defined block copolymer consisting of polyethylene and syndiotactic polypropylene segments with narrow polydispersity ($M_w/M_n < 1.20$). In addition, a new A−B diblock polymer consisting of crystalline and amorphous segments, polyethylene-*b*-poly(ethylene-*co*-propylene), was also synthesized. After preparation of the first PE block segment by the same procedure, the second monomer, ethylene/propylene gas feed (25/75 L/h), was started to produce a sequential poly-(ethylene-*co*-propylene) segment. The resulting block copolymer with a high molecular weight ($M_n = 211\,000$) and narrow polydispersity ($M_w/M_n = 1.16$) contained 6.4 mol % of propylene.

(22) Interestingly, a titanium FI Catalyst having a chlorine adjacent to the imine nitrogen, bis[*N*-(3-*tert*-butylsalicylidene)-2-chloroanilinato]titanium(IV) dichloride, also promoted ethylene polymerization at 25 °C to produce polyethylene having narrow polydispersity (1.23), implying that the β-hydrogen fixation is potentially achieved by any substituent possessing lone-pair electrons.

Table 6. Synthesis of Various Block Copolymers

entry	prepolymer		diblock copolymer			triblock copolymer		
	1st block	$M_n{}^a$, $M_w/M_n{}^a$	2nd block	$M_n{}^a$, $M_w/M_n{}^a$	propylene[b] contents	3rd block	$M_n{}^a$, $M_w/M_n{}^a$	propylene[b] contents
1	PE[c]	115 000, 1.10	PP[d]	136 000, 1.15	16.1			
2	PE	115 000, 1.10	E/P[e]	211 000, 1.16	6.4			
3	PE	115 000, 1.10	E/P	211 000, 1.16	6.4	PP	235 000, 1.15	14.1
4	PE	115 000, 1.10	E/P	211 000, 1.16	6.4	PE	272 000, 1.14	6.6

[a] Determined by GPC using polypropylene calibration. [b] Total propylene contents (mol %). Determined by NMR. [c] Polyethylene. [d] Polypropylene. [e] Ethylene–propylene random copolymer.

Likewise, polyethylene-*b*-poly(ethylene-*co*-propylene)-*b*-syndiotactic polypropylene (entry 3) and polyethylene-*b*-poly-(ethylene-*co*-propylene)-*b*-polyethylene[23] (entry 4) triblock copolymers were also prepared for the first time using the complex **1**/MAO catalyst system by the sequential addition of the monomers. The peak melting temperatures (T_m) of the block copolymers are 131 °C (entry 1), 123 °C (entry 2), 123 °C (entry 3), and 120 °C (entry 4), the T_m value being lower than the corresponding homopolyethylene (133 °C) and homopolypropylene (137 °C). Thus, the usefulness of the catalyst system for the synthesis of a wide array of block copolymers previously unavailable with Ziegler–Natta type catalysts has been demonstrated. The block copolymers produced by the catalyst system are anticipated to display novel properties and uses for high-performance polymers.

Experimental Section

General Comments. Syntheses. Ligand syntheses were carried out under nitrogen in oven-dried glassware. All manipulations of complex syntheses were performed with exclusion of oxygen and moisture under argon using standard Schlenk techniques in oven-dried glassware.

Materials. Dried solvents (diethyl ether, dichloromethane, and *n*-hexane) used for complex syntheses were purchased from Wako Pure Chemical Industries, Ltd., and used without further purification. Toluene used as a polymerization solvent (Wako Pure Chemical Industries, Ltd.) was dried over Al_2O_3 and degassed by bubbling with nitrogen gas. 3-*tert*-Butylsalicylaldehyde and aniline derivatives for ligand synthesis were obtained from Aldrich Chemical Co., Inc., Wako Pure Chemical Industries, Ltd., Acros Organics, or Tokyo Kasei Kogyo Co., Ltd. An *n*-butyllithium *n*-hexane solution and dried *n*-pentane were purchased from Kanto Chemical Co., Inc. $TiCl_4$ and Cp_2ZrCl_2 (Wako Pure Chemical Industries, Ltd.) were used as received. Ethylene and propylene were obtained from Sumitomo Seika Co. and Mitsui Chemicals, Inc., respectively. Bis[*N*-(3-*tert*-butylsalicylidene)anilinato]-titanium(IV) dichloride (**8**) was synthesized according to the previously described procedure.[16b]

Cocatalysts. Methylalmoxane (MAO) was purchased from Albemarle as a 1.2 M of a toluene solution, and the remaining trimethylaluminum was evaporated in vacuo prior to use.

Ligand and Complex Analyses. ^{1}H NMR spectra were recorded on a JEOL270 or an NEC-LA500 spectrometer at ambient temperatures. Chemical shifts for ^{1}H NMR were referenced to an internal solvent resonance and reported relative to tetramethylsilane. FD-MS spectra were recorded on an SX-102A instrument from Japan Electron Optics Laboratory Co., Ltd. Elemental analysis for C, H, and N was carried out by a CHNO type analyzer from Helaus Co.

Polymer Characterization. ^{13}C or ^{1}H NMR data for polyethylenes and block copolymers were obtained using *o*-dichlorobenzene with 20% benzene-d_6 as a solvent at 120 °C. M_n and M_w/M_n values of polymers

were determined using a Waters 150-C gel permeation chromatograph equipped with three TSKgel columns (two sets of TSKgelGMH$_{HR}$-H(S)HT and TSKgelGMH$_6$-HTL) at 145 °C using polyethylene or polypropylene calibration. *o*-Dichlorobenzene was employed as a solvent at a flow rate of 1.0 mL/min. Transition melting temperatures (T_m) of the polymers were determined by DSC with a Shimadzu DSC-60 differential scanning calorimeter, measured upon reheating the polymer sample to 200 °C at a heating rate of 10 °C/min. Propylene contents of the copolymers were determined by ^{13}C NMR analyses.

Preparation of Bis[*N*-(3-*tert*-butylsalicylidene)-2,3,4,5,6-pentafluoroanilinato]titanium(IV) Dichloride (1). Ligand Synthesis. To a stirred mixture of 3-*tert*-butylsalicylaldehyde (7.50 g, 98% purity, 41.2 mmol) and 2,3,4,5,6-pentafluoroaniline (9.06 g, 49.5 mmol) in toluene (100 mL) was added *p*-toluenesulfonic acid (ca. 20 mg) at room temperature. The resulting mixture was stirred at reflux temperature for 4 h, and concentration of the reaction mixture in vacuo afforded a crude imine compound. Purification by column chromatography on silica gel using *n*-hexane/AcOEt (100/1) as eluent gave *N*-(3-*tert*-butylsalicylidene)-2,3,4,5,6-pentafluoroaniline (**a**) (13.98 g, 40.7 mmol) as yellow crystals in 98% yield: ^{1}H NMR (CDCl$_3$) δ 1.46 (s, 9H, ^{t}Bu), 6.91 (t, $J = 7.8$ Hz, 1H, aromatic-H), 7.23–7.26 (m, 1H, aromatic-H), 7.47 (dd, $J = 7.7$, 1.5 Hz, 1H, aromatic-H), 8.81 (s, 1H, CH=N), 12.88 (s, 1H, OH).

Complex Synthesis. To a stirred solution of *N*-(3-*tert*-butylsalicylidene)-2,3,4,5,6-pentafluoroaniline (4.87 g, 14.0 mmol) in dried diethyl ether (50 mL) at −78 °C was added a 1.52 M *n*-butyllithium/*n*-hexane solution (9.21 mL, 14.0 mmol) dropwise over a 10-min period. The solution was allowed to warm to room temperature and stirred for 2 h. The resulting solution was added dropwise over a 10-min period to a 0.5 M *n*-heptane solution of TiCl$_4$ (14.0 mL, 7.00 mmol) in dried diethyl ether (50 mL) at −78 °C. The mixture was allowed to warm to room temperature and stirred for 18 h. Concentration of the reaction mixture in vacuo gave a crude product. Dried CH$_2$Cl$_2$ (80 mL) was added to the crude product, and the mixture was stirred for 15 min and then filtered. The solid residue was washed with dried CH$_2$Cl$_2$ (30 mL × 3), and the combined organic filtrates were concentrated in vacuo to afford a brown solid. Diethyl ether (30 mL) and *n*-hexane (120 mL) were added to the solid, and the mixture was stirred for 90 min and then filtered. The resulting solid was washed with *n*-hexane (20 mL × 3) and dried in vacuo to give complex **1** (4.03 g, contains 33 mol % of diethyl ether, 4.86 mmol) as a reddish brown solid in 69% yield.

Compound **1**, as reddish brown crystals: ^{1}H NMR (CDCl$_3$) δ 1.35 (s, 18H, ^{t}Bu), 7.02 (t, $J = 7.6$ Hz, 2H, aromatic-H), 7.29 (dd, $J = 7.6$, 1.6 Hz, 2H, aromatic-H), 7.64 (dd, $J = 7.6$, 1.6 Hz, 2H, aromatic-H), 8.22 (s, 2H, CH=N), 1.21 (t, $J = 7.0$ Hz, (CH$_3$CH$_2$)O), 3.48 (q, $J = 7.0$ Hz, (CH$_3$CH$_2$)O); FD-MS, 802 (M$^+$). Anal. Found: C, 51.71; H, 4.04; N, 3.79. Calcd for TiC$_{34}$H$_{26}$N$_2$O$_2$F$_{10}$Cl$_2$·^{1}/$_3$Et$_2$O: C, 51.25; H, 3.57; N, 3.38.

Preparation of Bis[*N*-(3-*tert*-butylsalicylidene)-2,4,6-trifluoroanilinato]titanium(IV) Dichloride (2). Ligand **b**, *N*-(3-*tert*-butylsalicylidene)-2,4,6-trifluoroaniline, as an orange oil: ^{1}H NMR (CDCl$_3$) δ 1.47 (s, 9H, ^{t}Bu), 6.75–6.91 (m, 3H, aromatic-H), 7.23 (dd, $J = 7.6$, 1.6 Hz, 1H, aromatic-H), 7.43 (dd, $J = 7.6$, 1.6 Hz, 1H, aromatic-H),

(23) Because propylene is present in the polymerization system during the creation of the third segment, the third segment is actually an ethylene/propylene random copolymer with low propylene content (ca. 7 mol %).

8.83 (s, 1H, CH=N), 13.35 (s, 1H, OH). Compound **2**, as dark red crystals: ¹H NMR (CDCl₃) δ 1.31 (s, 18H, ᵗBu), 6.26 (bs, 2H, aromatic-H), 6.65−6.74 (m, 2H, aromatic-H), 6.96 (t, J = 7.8 Hz, 2H, aromatic-H), 7.25 (dd, J = 7.9, 1.6 Hz, 2H, aromatic-H), 7.56 (dd, J = 7.9, 1.6 Hz, 2H, aromatic-H), 8.18 (s, 2H, CH=N); FD-MS, 730 (M⁺). Anal. Found: C, 55.22; H, 4.07; N, 3.71. Calcd for TiC₃₄H₃₀N₂O₂F₆Cl₂: C, 55.83; H, 4.13; N, 3.83.

Preparation of Bis[*N*-(3-*tert*-butylsalicylidene)-2,6-difluoroanilinato]titanium(IV) Dichloride (3). Ligand **c**, *N*-(3-*tert*-butylsalicylidene)-2,6-difluoroaniline, as orange crystals: ¹H NMR (CDCl₃) δ 1.47 (s, 9H, ᵗBu), 6.88 (t, J = 7.6 Hz, 1H, aromatic-H), 6.95−7.16 (m, 3H, aromatic-H), 7.24 (dd, J = 7.7, 1.4 Hz, 1H, aromatic-H), 7.42 (dd, J = 7.7, 1.4 Hz, 1H, aromatic-H), 8.86 (s, 1H, CH=N), 13.50 (s, 1H, OH). Compound **3**, as brown crystals: ¹H NMR (CDCl₃), δ 1.26 (s, 18H, ᵗBu), 6.44−6.51 (m, 2H, aromatic-H), 6.87−7.02 (m, 6H, aromatic-H), 7.25 (dd, J = 7.5, 1.9 Hz, 2H, aromatic-H), 7.50 (dd, J = 7.5, 1.9 Hz, 2H, aromatic-H), 8.21 (s, 2H, CH=N), 1.21 (t, J = 7.0 Hz, (CH₃CH₂)O), 3.48 (q, J = 7.0 Hz, (CH₃CH₂)O); FD-MS, 694 (M⁺). Anal. Found: C, 58.89; H, 5.33; N, 3.51. Calcd for TiC₃₄H₃₂N₂O₂F₄-Cl₂·0.8Et₂O: C, 59.20; H, 5.34; N, 3.71.

Preparation of Bis[*N*-(3-*tert*-butylsalicylidene)-2-fluoroanilinato]titanium(IV) Dichloride (4). Ligand **d**, *N*-(3-*tert*-butylsalicylidene)-2-fluoroaniline, as a yellow oil: ¹H NMR (CDCl₃) δ 1.47 (s, 9H, ᵗBu), 6.87 (t, J = 7.8 Hz, 1H, aromatic-H), 7.12−7.30 (m, 5H, aromatic-H), 7.41 (d, J = 7.6 Hz, 1H, aromatic-H), 8.70 (s, 1H, CH=N), 13.70 (s, 1H, OH). Compound **4**, as dark red crystals: ¹H NMR (CDCl₃), δ 1.31(s, 18H, ᵗBu), 6.70−7.35 (m, 12H, aromatic-H), 7.42 (dd, J = 7.8, 1.6 Hz, 2H, aromatic-H), 8.12 (s, 2H, CH=N); FD-MS, 658 (M⁺). Anal. Found: C, 61.93; H, 5.17; N, 4.09. Calcd for TiC₃₄H₃₄N₂O₂F₂-Cl₂: C, 61.93; H, 5.20; N, 4.25.

Preparation of Bis[*N*-(3-*tert*-butylsalicylidene)-3,4,5-trifluoroanilinato]titanium(IV) Dichloride (5). Ligand **e**, *N*-(3-*tert*-butylsalicylidene)-3,4,5-trifluoroaniline, as yellow crystals: ¹H NMR (CDCl₃) δ 1.46 (s, 9H, ᵗBu), 6.87−6.99 (m, 3H, aromatic-H), 7.43 (d, J = 7.8 Hz, 1H, aromatic-H), 8.54 (s, 1H, CH=N), 13.19 (bs, 1H, OH). Compound **5**, as dark red crystals: ¹H NMR (CDCl₃), δ 1.23−1.61 (m, 18H, ᵗBu), 6.64−6.69 (m, 4H, aromatic-H), 6.93−7.33 (m, 4H, aromatic-H), 7.56−7.72 (m, 2H, aromatic-H), 8.03−8.09 (m, 2H, CH=N); FD-MS, 730 (M⁺). Anal. Found: C, 55.96; H, 4.00; N, 3.56. Calcd for TiC₃₄H₃₀N₂O₂F₆Cl₂: C, 55.83; H, 4.13; N, 3.83.

Preparation of Bis[*N*-(3-*tert*-butylsalicylidene)-3,5-difluoroanilinato]titanium(IV) Dichloride (6). Ligand **f**, *N*-(3-*tert*-butylsalicylidene)-3,5-difluoroaniline, as a yellow oil: ¹H NMR (CDCl₃) δ 1.46 (s, 9H, ᵗBu), 6.67−7.44 (m, 6H, aromatic-H), 8.56 (s, 1H, CH=N), 13.30 (s, 1H, OH). Compound **6**, as dark red crystals: ¹H NMR (CDCl₃), δ 1.32−1.62 (m, 18H, ᵗBu), 6.33−7.33 (m, 10H, aromatic-H), 7.52−7.70 (m, 2H, aromatic-H), 8.03−8.10 (m, 2H, CH=N); FD-MS, 694 (M⁺). Anal. Found: C, 58.83; H, 4.91; N, 3.78. Calcd for TiC₃₄H₃₂N₂O₂-F₄Cl₂: C, 58.72; H, 4.64; N, 4.03.

Preparation of Bis[*N*-(3-*tert*-butylsalicylidene)-4-fluoroanilinato]titanium(IV) Dichloride (7). Ligand **g**, *N*-(3-*tert*-butylsalicylidene)-4-fluoroaniline, as an orange oil: ¹H NMR (CDCl₃) δ 1.47 (s, 9H, ᵗBu), 6.88 (t, J = 7.6 Hz, 1H, aromatic-H), 7.04−7.41 (m, 6H, aromatic-H), 8.59 (s, 1H, CH=N), 13.76 (s, 1H, OH). (**7**); as brown crystals: ¹H NMR (CDCl₃), δ 1.07−1.61 (m, 18H, ᵗBu), 6.71−7.67 (m, 14H, aromatic-H), 7.96−8.13 (m, 2H, CH=N); FD-MS, 658 (M⁺). Anal. Found: C, 62.04; H, 5.30; N, 3.77. Calcd for TiC₃₄H₃₄N₂O₂F₂Cl₂: C, 61.93; H, 5.20; N, 4.25.

X-ray Crystallography. Single crystals of complexes **1** and **3** suitable for an X-ray analysis were grown from a saturated pentane/CH₂Cl₂ solution. The X-ray structure analyses data were collected using a Rigaku RAXIS-RAPID imaging plate diffractometer (complex **1**) or a Rigaku AFC7R diffractometer (complex **3**). The structure was solved by direct method[24] and expanded using Fourier techniques. The non-hydrogen atoms were refined anisotropically. Hydrogen atoms were

Table 7. Summary of Crystallographic Data for Complexes **1** and **3**

complex	**1**·CH₂Cl₂	**3**·C₅H₁₂
	A. Crystal Data	
empirical formula	C₃₅H₂₈Cl₄F₁₀N₂O₂Ti	C₂₉H₄₄Cl₂F₄N₂O₂Ti
fw	888.31	767.59
crystal color, habit	red, platelet	red, platelet
crystal size (mm)	0.40 × 0.35 × 0.07	0.30 × 0.20 × 0.05
crystal system	monoclinic	monoclinic
a (Å)	11.6786(2)	18.447(2)
b (Å)	25.6347(9)	24.188(5)
c (Å)	12.3467(1)	8.538(1)
β (deg)	92.254(4)	91.557(8)
V (Å³)	3693.5(1)	3808.3(10)
space group	P2₁/n (No. 14)	P2₁/n (No. 14)
Z	4	4
D_calcd (g/cm)	1.597	1.213
F₀₀₀	1792.00	1432.00
μ (Mo Kα) (cm⁻¹)	6.07	4.13
	B. Data Collection	
λ (Mo Kα) (Å)	0.71069	0.71069
T (°C)	−160.0	25.0
2θ_max	59.9	55.0
no. of total reflns	32621	106.36
no. of unique reflns	9925 (R_int = 0.076)	8740 (R_int = 0.019)
	C. Structure Solution and Refinement	
no. observations	9917 (I > 3.00σ(I))	6988 (I > 2.00σ(I))
no. variables	487	451
refln/parameter ratio	20.36	15.49
residuals: R, Rw	0.084, 0.073	0.053, 0.050
goodness of fit indicator	1.11	0.81
max shift/error in final cycle	0.001	0.11
max peak in final diff map (e⁻/Å³)	0.02	0.30
min peak in final diff max (e⁻/Å³)	−0.02	−0.37

included but not refined. All calculations were performed using the teXan[25] crystallographic software package of Molecular Structure Corp. Experimental data for the X-ray diffraction analyses of complexes **1** and **3** are summarized in Table 7.

DFT Calculations.[26] All calculations were performed at the gradient-corrected density functional BLYP level by means of the Amsterdam density functional (ADF) program. We used the triple ζ STO basis set for the zirconium and the double ζ STO basis set for the other atoms to calculate the optimized geometries. For Mulliken population analysis, the triple ζ STO basis set for the zirconium and the double ζ plus polarization STO basis set for the other atoms were used, and the quasirelativistic correction was also added. The classical electrostatic energies between the β-hydrogen and the nearest neighboring fluorine were estimated by the following equation:

$$ES = q(H_\beta)q(F)/r(F-H_\beta)$$

Here $q(H_\beta)$ and $q(F)$ stand for Mulliken charges of the β-hydrogen and the nearest neighboring fluorine, respectively, and $r(F-H_\beta)$ is the distance between those two atoms. All units are in atomic unit.

Ethylene Polymerization. General Procedure. Ethylene polymerization was carried out under atmospheric pressure in toluene in a

(24) Complex **1**, SIR97: Altomale, A.; Burla, M. C.; Camalli, M.; Cascarano, M.; Giacovazzo, C.; Guagliardi, A.; Moliterni, A. G. G.; Polidori, G.; Spagna, R. *J. Appl. Cryst.* **1999**, *32*, 115−119. Complex **3**, SIR92: Altomale, A.; Burla, M. C.; Camalli, M.; Cascarano, M.; Giacovazzo, C.; Guagliardi, A.; Polidori, G. *J. Appl. Cryst.* **1994**, *27*, 435−436.

(25) TeXan: Crystal Structure Analysis Package, Molecular Structure Corp. (1985 & 1992).

(26) (a) Fonseca Guerra, C.; Snijders, J. G.; te Velde, G.; Baerends, E. J. *Theor. Chem. Acc.* **1998**, *99*, 391−403. (b) Deng, L.; Ziegler, T.; Woo, T. K.; Margl, P.; Fan, L. *Organometallics* **1998**, *17*, 3240−3253. (c) R. S. Mulliken, *J. Chem. Phys.* **1955**, *23*, 1833.

500-mL glass reactor equipped with a propeller-like stirrer. Toluene (250 mL) was introduced into the nitrogen-purged reactor and stirred (600 rpm). The toluene was thermostated to a prescribed polymerization temperature, and then the ethylene gas feed (100 L/h) was started. After 10 min, polymerization was initiated by adding a toluene solution of MAO (1.0 M. 1.25 mL) and then a toluene solution of a complex into the reactor with stirring (600 rpm). After a prescribed time, *sec*-butyl alcohol (10 mL) was added to terminate the polymerization. To the resulting mixture, methanol (250 mL) and concentrated HCl (2 mL) were added. The polymer was collected by filtration, washed with methanol (200 mL), and dried in vacuo at 80 °C for 10 h.

Polymerization Using Diluted Ethylene with N_2 (Table 3 and Figure 7). Polymerization using diluted ethylene with N_2 was performed by using ethylene$-N_2$ mixed gas in place of ethylene gas [complex **1**: ethylene/N_2 feed 2 L/50 L/h (25, 50 °C), 5 L/50 L/h (75 °C) (Table 3)] [complex **2**: ethylene, 10 L/h; N_2, 50 L/h (Figure 7)] using the same type of equipment and the same manner for the general procedure described above, except for stirring (400 rpm).

Postpolymerization Method (Figure 11). The postpolymerization method was carried out using the same type equipment under atmospheric pressure. Toluene (250 mL) was introduced into the nitrogen-purged reactor and stirred (300 rpm). The toluene was kept at 25 °C, and then the ethylene gas feed (100 L/h) was started. After 5 min, the ethylene gas feed was stopped and the toluene solution was kept under N_2. To the resulting toluene solution were added toluene solutions of MAO (1.0 M, 2.5 mL) and complex **1** (2 mM, 5.0 mL) to start ethylene polymerization.

Entries 1−5. After a prescribed time, *sec*-butyl alcohol (10 mL) was added to terminate the polymerization. Polymer purification and isolation were performed using the same method as the general procedure.

Entry 6. After 65 min, the ethylene gas feed (20 L/h) was initiated to perform postpolymerization. After 2 min, *sec*-butyl alcohol (10 mL) was added to terminate the polymerization. Polymer purification and isolation were performed using the same method as described in the general procedure.

Synthetic Procedure for Block Copolymers. Block copolymers were synthesized using the same type of equipment under atmospheric pressure.

PE−PP Diblock Copolymer (Table 6, Entry 1). Toluene (250 mL) was introduced into the nitrogen-purged reactor and stirred (300 rpm). The toluene was kept at 25 °C, and then the ethylene gas feed (100 L/h) was started. After 5 min, the ethylene gas feed was stopped and the toluene solution was kept under N_2 for 5 min. To the resulting toluene solution were added toluene solutions of MAO (1.0 M, 2.5 mL) and complex **1** (2 mM, 5.0 mL) to produce the polyethylene (PE) segment. After 5 min, the propylene gas feed (30 L/h) was initiated. After 20 min, the propylene gas feed was stopped, and the mixture was stirred for 280 min to create the sequential polypropylene (PP) segment. *sec*-Butyl alcohol (10 mL) was added to terminate the polymerization. The resulting mixture was added to acidic methanol (1000 mL), including concentrated HCl (2 mL). The polymer was collected by filtration, washed with methanol (200 mL), and dried in vacuo at 80 °C for 10 h.

PE−E/P Diblock Copolymer (Table 6, Entry 2). After the preparation of the polyethylene segment using the same method for the preparation of the polyethylene segment for PE−PP diblock copolymer, the ethylene/propylene mixed gas feed (ethylene 25 L/h, propylene 75 L/h) was initiated. After 3 min, the ethylene/propylene mixed gas feed was stopped, and the mixture was stirred for 3 min to create the sequential ethylene/propylene random copolymer (E/P) segment. *sec*-Butyl alcohol (10 mL) was added to terminate the polymerization. The resulting mixture was added to acidic methanol (1000 mL) including concentrated HCl (2 mL). The polymer was collected by filtration, washed with methanol (200 mL), and dried in vacuo at 130 °C for 10 h.

PE−E/P−PP Triblock Copolymer (Table 6, Entry 3). After the preparation of the polyethylene-*b*-poly(ethylene-*co*-propylene) segment using the same method for the preparation of PE−E/P diblock copolymer, the propylene gas feed (30 L/h) was initiated. After 20 min, the propylene gas feed was stopped, and the mixture was stirred for 280 min to create the sequential polypropylene (PP) segment. *sec*-Butyl alcohol (10 mL) was added to terminate the polymerization. The resulting mixture was added to acidic methanol (1000 mL) including concentrated HCl (2 mL). The polymer was collected by filtration, washed with methanol (200 mL), and dried in vacuo at 130 °C for 10 h.

PE−E/P−PE Triblock Copolymer (Table 6, Entry 4). After the preparation of the polyethylene-*b*-poly(ethylene-*co*-propylene) segment using the same method for the preparation of PE-E/P diblock copolymer, the ethylene gas feed (100 L/h) was initiated to create the sequential polyethylene (PE) segment. After 1 min, *sec*-butyl alcohol (10 mL) was added to terminate the polymerization. The resulting mixture was added to acidic methanol (1000 mL) including concentrated HCl (2 mL). The polymer was collected by filtration, washed with methanol (200 mL), and dried in vacuo at 130 °C for 10 h.

Conclusion

In conclusion, we have developed a new series of titanium complexes having fluorine-containing phenoxy−imine chelate ligands, some titanium FI Catalysts, which are effective catalysts for the living polymerization of ethylene using MAO as a cocatalyst. The catalyst systems display very high activities (TOF value > 20 000 min^{-1} atm^{-1}) and create high molecular weight polyethylenes (M_n > 400 000) with extremely narrow polydispersities (M_w/M_n < 1.20) at very high polymerization temperatures (25−50 °C). DFT calculations suggest that the fluorine adjacent to the imine nitrogen of an active species, for ethylene polymerization, interacts with a β-hydrogen of a polymer chain to prevent the β-hydrogen transfer, an interaction providing a new breakthrough for accomplishing high-temperature living ethylene polymerization. Using the FI Catalyst possessing *N*-(3-*tert*-butylsalicylidene)pentafluoroaniline ligands/ MAO system, a number of new block copolymers such as polyethylene-*b*-poly(ethylene-*co*-propylene)-*b*-syndiotactic polypropylene triblock copolymer have been successfully prepared. The results introduced herein together with our previous results show that group 4 transition metal complexes having phenoxy-imine chelate ligands, FI Catalysts, possess high potential for olefin polymerization, resulting in novel polymers that are anticipated to exhibit new properties and uses.

Supporting Information Available: Full crystallographic data and DFT calculation for complexes **1** and **3**, detailed synthesis data for complexes **2**−**7**, and ^{13}C NMR spectrum and GPC and DSC charts of the polymers. This material is available free of charge via the Internet at http://pubs.acs.org.

JA0117581